



## Impact of cathode channel depth on performance of direct methanol fuel cells

Sang Youp Hwang<sup>a,b</sup>, Han-Ik Joh<sup>a</sup>, M. Aulice Scibioh<sup>a</sup>, Sang-Yeop Lee<sup>a</sup>, Soo-Kil Kim<sup>a</sup>,  
Tai Gyu Lee<sup>b,\*</sup>, Heung Yong Ha<sup>a,\*</sup>

<sup>a</sup> Center for Fuel Cell Research, Korea Institute of Science and Technology, 39-1 Hawolgok-dong, Seongbuk-gu, Seoul 136-791, Republic of Korea

<sup>b</sup> Department of Chemical Engineering, Yonsei University, 134 Sinchon-dong, Seodaemun-gu, Seoul 120-749, Republic of Korea

### ARTICLE INFO

#### Article history:

Received 14 January 2008

Received in revised form 27 February 2008

Accepted 7 April 2008

Available online 26 April 2008

#### Keywords:

Direct methanol fuel cell

Bipolar plate

Cathode channel depth

Mass transport

Linear velocity

Operational stability

### ABSTRACT

The major functions of bipolar plates in fuel cell systems are to transport effectively the reactants and the products to and from the electrodes, and to collect efficiently the current that is generated in the cell. A suitable approach to enhance the performance of the bipolar plate with respect to mass transport is to optimize the channel dimension and shape. In this study, the impact of the cathode channel depth on the performance of direct methanol fuel cells is investigated. When the channel depth of the bipolar plate is decreased from 1.0 to 0.3 mm, the cell performance increases and also remains stable during continuous operation of the cell. The decreased channel depth leads to an increase in the linear velocity of the reactants and products at a given volumetric flow rate that, in turn, facilitates their mass transport. Furthermore, in smaller channels (shallower channels), the pressure drop is increased and this can lead to an increase in partial pressure of the oxygen, which has a positive impact on cell performance. The effect of cathode channel depth on the transport behaviour of reactants and products is studied by means of employing the transparent plates, which are designed to monitor visually the flow of reactants and products in the cathode channels. Additionally, the pressure drop and linear velocity in the cell is calculated by using a computational fluid dynamics (CFD) technique.

© 2008 Elsevier B.V. All rights reserved.

### 1. Introduction

Fuel cells are effective energy conversion devices, in which the occurrence of an electrochemical reaction between a fuel and an oxidant can convert the chemical energy of the fuel directly into electrical energy. The direct methanol fuel cells (DMFCs), which utilizes methanol as a fuel, have been considered as a promising power source for portable electronic devices and automobiles. Methanol has a high energy specific, superior chemical stability, and is easy to transport and store. Because of these properties, the DMFC system is simple and compact compared with other fuel cell systems [1–5].

Many strategies have been proposed to enhance DMFC performance. These include the use of Pt–Ru bimetallic catalysts to promote the kinetics of methanol oxidation [6], the fabrication of composite membranes [7] or the modification of Nafion membranes to reduce methanol crossover [8], the addition of a microporous layer in the membrane–electrode assembly (MEA) [9], and fabrication of the MEA by the decal method [10]. Besides the

abovementioned approaches, there are other possibilities available to improve cell performance. One approach is to optimize the channel dimensions of the bipolar plates as this can have a positive impact on mass transport phenomena. The functions of the bipolar plates are to transport effectively both the reactants and the products to and from the electrodes, in addition to collecting the electric current in an efficient way. Therefore, it is a necessity to optimize the plates with regard to the type of flow-field, the type of materials, and the relative sizes and cross-sectional areas of the channels and ribs [11–13].

Most of the previous research into the development of flow-fields for DMFCs has focused mainly on the optimization or modification of the anode plates. For instance, Yang and Zhao [14] investigated the effect of channel type on the performance of a cell and reported that a single serpentine flow-field gave better performance than a parallel flow-field. The reason for the higher performance of the former flow-field was attributed to the effective removal of the anode product, carbon dioxide, in the flow-field. In addition, anode channel depth was correlated with cell performance [15–17]. The results showed better performance with the shallower channel depth at the same open ratio was due to efficient mass transport between the gas-diffusion layer (GDL) and the flow-field with the increased linear (flow) velocity of the reactant. From that study, it was understood that there must be an optimum

\* Corresponding author. Tel.: +82 2 2123 5751; fax: +82 2 312 6401.

\*\* Corresponding author. Tel.: +82 2 958 5275; fax: +82 2 958 5199.

E-mail addresses: [teddy.lee@yonsei.ac.kr](mailto:teddy.lee@yonsei.ac.kr) (T.G. Lee),  
[hyha@kist.re.kr](mailto:hyha@kist.re.kr), [hyha88@hotmail.com](mailto:hyha88@hotmail.com) (H.Y. Ha).

channel depth; on the other hand, too shallow a channel depth had a negative impact on the removal of carbon dioxide [15,16].

Wong et al. [16] also studied the impact of the anode channel width on cell behaviour and concluded that a narrower channel depth resulted in better performance, which could be due to the effective mass transport with increased linear velocity of the methanol solutions, as discussed above. Furthermore, the authors showed that as the channel width decreased below 580  $\mu\text{m}$ , the cell performance started to decline. This is presumably because of the increased residence time of carbon dioxide inside the channel that is likely to block the active surface area of the membrane–electrode assembly. In another study, Yoon et al. [18] examined the performance of a cell by altering the area ratio between the channel and the rib. In that study, since the rib acted as a current-collector, the increased rib portion could lead to better conductivity of the bipolar plates. It was, however, concluded that a higher portion of channel area can be beneficial to the high-power operation of a cell, because the mass transport has a more pronounced effect on cell performance than that of electric conductivity.

As most of the studies have focused mainly on the anode side, it proved difficult to find any experimental reports that dealt with the cathode side, particularly for the DMFC. In order to reduce the stack volume of a DMFC, it is essential to minimize the cathode channel depth. Nevertheless, it should be mentioned that a shallower cathode channel depth is more likely to cause a larger pressure drop in a cell and that can render higher power consumption to the air blower, which in turn, results in increasing parasitic power losses [11]. Therefore, an optimization of the cathode channel dimension has become essential to make thinner DMFC stacks.

This study investigates the effects of cathode channel depth on the performance of a DMFC. First, the pressure drop and linear velocity of various channel depths are calculated by using a computational fluid dynamics (CFD) technique. In order to elucidate the relationship between the channel depth and the performance of a fuel cell, a series of experiments are conducted by changing the air flow rate, applying back pressure and monitoring the stability of performance during the operation of a cell. In addition, the behaviour of air and water in the cathode channel are monitored by using the transparent plates.

## 2. Experimental

The MEAs were fabricated via the procedure described below. Gas-diffusion layers both for the anode and the cathode were fabricated by coating 2.0  $\text{mg cm}^{-2}$  of a Vulcan carbon layer on carbon paper (Toray, TGP-H-060, 20 wt% PTFE) [19,20]. Pt–Ru (1:1) and Pt black (Johnson Matthey Co.) catalysts were used for the anode and the cathode, respectively. The catalyst ink solutions were prepared by taking an appropriate amount of catalyst in de-ionized water and the mixture was ultrasonicated for 5 min. Subsequently, 5 wt% Nafion ionomer and *iso*-propyl alcohol were added to the mixture and it was further ultrasonicated for 5 min to obtain a homogeneous dispersion of the catalysts. Then, the prepared ink solution was directly sprayed on to both sides of a Nafion 115 membrane (Dupont) with an area of 3.3  $\text{cm} \times 3.3 \text{ cm}$  to fabricate catalyst-coated membranes (CCMs). The catalyst loading both on the anode and the cathode was 3  $\text{mg cm}^{-2}$ . The MEAs were fabricated by placing carbon-coated GDLs on either side of the CCM and then pressed at 8 MPa and 140  $^{\circ}\text{C}$  for 5 min.

Plates with three-serpentine channels were employed, each with dimensions of 1.0  $\text{mm} \times 1.0 \text{ mm}$  (depth  $\times$  width) for the anode and  $D \text{ mm} \times 1.0 \text{ mm}$  (depth  $\times$  width,  $D = 0.3, 0.5, 0.8, 1.0 \text{ mm}$ ) for the cathode, respectively. The open ratio of the channel to rib was fixed to 51% for all plates.

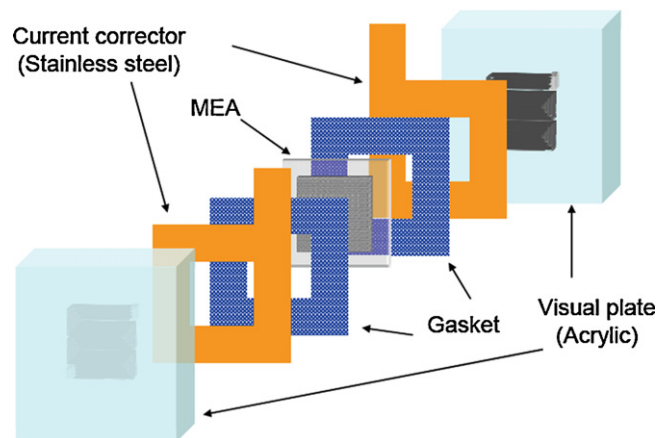


Fig. 1. Schematic diagram of cell assembly with transparent end-plates.

One molar of methanol solution was fed to the anode using a peristaltic pump, whereas air (dry or wet) was fed to the cathode. A single-cell test was carried out by connecting the cell to an electric load (WonA Tech, Korea) at a temperature of 80  $^{\circ}\text{C}$ . The effect of cathode channel depth and related phenomena on cell performance was investigated by varying the channel depth, flow rate, back pressure, and reactants stoichiometry. An electrochemical impedance spectroscopy (EIS) (IM 6, Zahner) study was carried out for a single cell DMFC by using the galvanostat mode under the operating conditions as mentioned above.

The transport behaviour of water, which is produced at the cathode depending on the depth of a channel, was monitored by the use of transparent acrylic plates [21]. The channel shape was similar to that in the graphite plates, but the channel depth varied from 0.5 and 1.0 mm. In order to have a clear visibility through the transparent plate and to collect the generated current, a stainless steel sheet was attached along the peripheral of the MEA, as shown in Fig. 1. This configuration enabled the visual monitoring of the electrode surface. A certain amount of current loss was inevitable due to the decreased contact area between the MEA and the current-collector. The behaviour of product water at the cathode was recorded with a video camera (see Fig. 2), with simultaneous measurement of the pressure drop and cell performance.

The pressure drop and linear velocity were calculated at various channel depths using a CFD technique (Star-CD) with governing

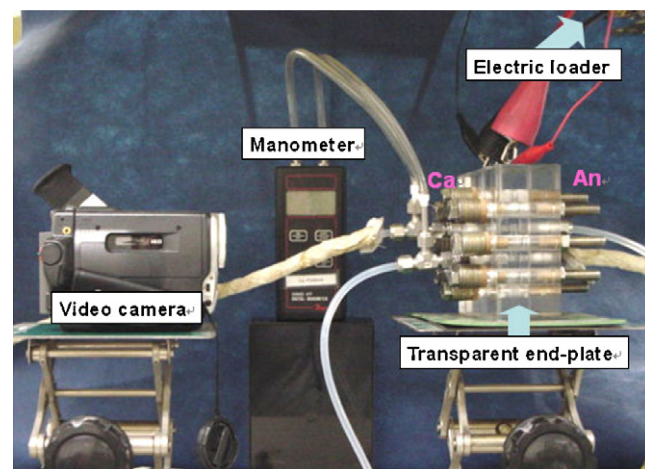


Fig. 2. Configuration of visual monitoring system. (Behaviour of water at cathode monitored with a camera through the transparent acrylic plate.)

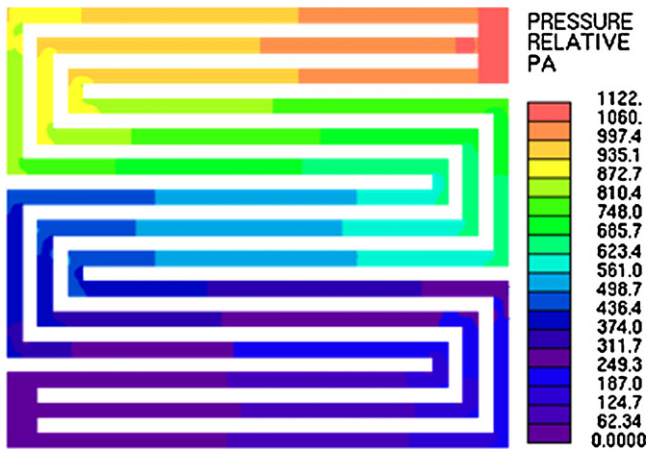


Fig. 3. Distribution of pressure and linear velocity at channel depth 1.0 mm.

Eqs. (1) and (2), assuming a constant viscosity and density under steady-state conditions:

$$\nabla \cdot (\rho \mathbf{v}) = 0 \quad (\text{continuity equation}) \quad (1)$$

$$\rho(\mathbf{v} \nabla \cdot \mathbf{v}) = -\nabla P + \mu \nabla^2 \mathbf{v} \quad (\text{Navier–Stokes equation}) \quad (2)$$

where  $\mathbf{v}$  is a velocity vector,  $P$  is the pressure,  $\rho$  is the density, and  $\mu$  is the viscosity. The values of density, viscosity and flow rate of the dry air used in this calculation were  $0.968 \text{ kg m}^{-3}$ ,  $2.08 \times 10^{-5} \text{ kg m}^{-1} \text{ s}^{-1}$  and 1250 sccm, respectively, at a cell operating temperature of  $80^\circ\text{C}$ .

### 3. Results and discussion

First, the pressure drop and linear velocity were calculated using a CFD code based on a single cell. The profiles of pressure in the channels with a depth of 1.0 mm are shown in Fig. 3. The internal pressure gradually declines from the inlet to the outlet along the channels. Curves summarizing the pressure drop and the average linear velocity in the channels as a function of channel depth are given in Fig. 4. As the channel depth decreases, the internal pressure and the linear velocity increases. The linear velocity can be defined as the volumetric flow rate divided by the cross-sectional area of a channel and is inversely proportional to the channel depth, which implies that the enhanced mass transfer occurs in the shallower channels [15,16,22,23].

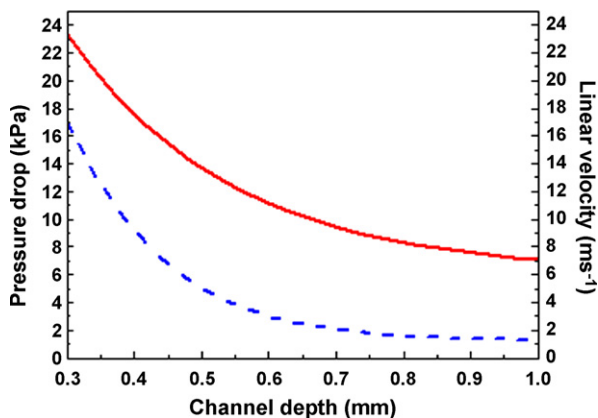


Fig. 4. Simulated results of pressure drop and linear velocity at different channel depths.

In order to evaluate the effect of cathode channel depth on the performance of a single cell various depths from 0.3 to 1.0 mm were tested, while the anode channel depth was fixed at 1.0 mm. One molar of methanol solution and humidified air were fed at the rate of  $5 \text{ ml min}^{-1}$  and 1250 sccm, respectively, to the anode and the cathode of a cell, which was operated at  $80^\circ\text{C}$  and atmospheric pressure. As shown in Fig. 5, the shallower cathode channel depth exhibits better performance; a decrease in depth from 1.0 to 0.3 mm results in an improvement of cell performance by nearly 17% at 0.4 V. In fact, the kinetics of the oxygen reduction at the cathode measured by impedance analysis (Fig. 5(b)) are not affected by the channel depth and the enhancement in performance is more pronounced in the higher current density region (see Fig. 5(a)), where the system is controlled by mass transfer. The superior performance with the shallower channel can be related to increased mass transfer of both the reactants and the products.

Wong et al. [15] noted that the linear velocity, and thus the Reynolds number ( $Re$ ), of a stream in the channels is likely to be affected by the channel depth, which in turn influences mass transport through the electrodes. That is, a decrease in the cross-sectional area of a channel by thinning the depth can lead to an increase in the linear velocity of the air inside the cathode channel (as well as the  $Re$  number), while the volumetric flow is maintained at the same rate. The  $Re$  numbers in the system shown in Fig. 5 are 740, 822, 987 and 1138 for a channel depth of 1.0, 0.8, 0.5 and 0.3 mm, respectively. Nevertheless, the  $Re$  numbers are still in the range of laminar flow, where the  $Re$  number does not have a direct relation with mass transport. Instead, the effect of linear velocity of the reactant may be better understood in terms of the Peclet number and the Sherwood number, i.e.,  $Pe = uL/D$ ,

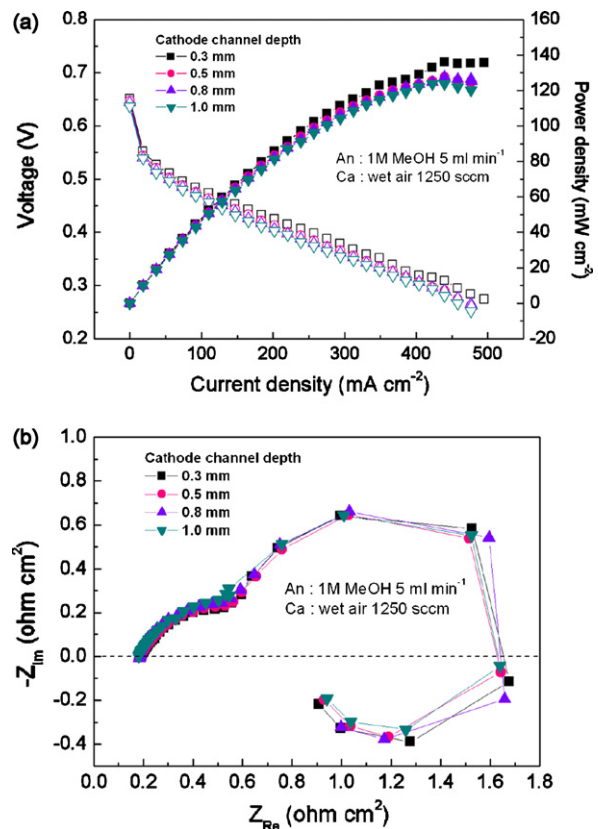
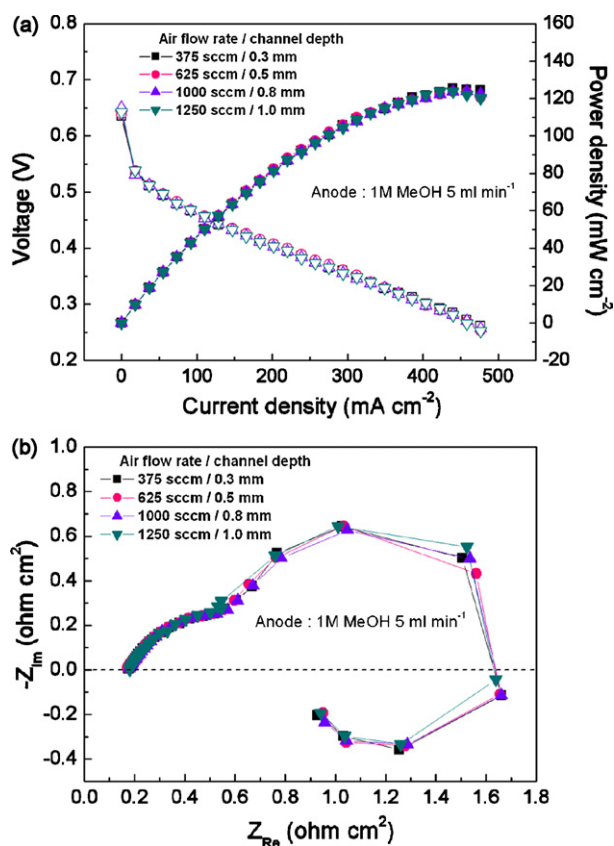


Fig. 5. (a) Performance of DMFC single cell at  $80^\circ\text{C}$  and (b) electrochemical impedance analysis for cell at  $80^\circ\text{C}$  with cathode channel depth varying from 0.3 to 1 mm. One molar of methanol and wet air fed at rate of  $5 \text{ cm}^3 \text{ min}^{-1}$  and 1250 sccm to anode and cathode, respectively.

$Sh = kL/D$ , where  $u$  = linear velocity ( $\text{m s}^{-1}$ ),  $L$  = characteristic length (m),  $D$  = diffusivity ( $\text{m}^2 \text{s}^{-1}$ ),  $k$  = mass-transfer coefficient ( $\text{m s}^{-1}$ ). The Sherwood number indicates the mass transport between the gas-diffusion layer and the channels. According to previous studies [17,24] that examined mass transport problems between the channels and the electrodes, the Peclet number increases on increasing the reactant velocity, which in turn increases the Sherwood number. Hence, in this investigation, we have inferred that an increase in the linear velocity can increase the Peclet number, which leads to enhanced mass transport through the electrodes by increasing the Sherwood number. A mathematical description of the relationships between the Peclet number and the Sherwood number and their effects on mass transport has been given by Yang et al. [17].

The effect of the linear velocity of the air at the cathode on the performance of a cell was investigated more precisely by conducting the following experiments. The linear velocities were maintained at a constant value regardless of the cathode channel depth by controlling the individual flow rates, viz., 1250, 1000, 625 and 375 sccm for a channel of 1.0, 0.8, 0.5 and 0.3 mm, respectively. The resulting linear velocity value is  $20.8 \text{ m s}^{-1}$  for all the channels and the corresponding cell performance is depicted in Fig. 6(a). The cells were operated at  $80^\circ\text{C}$  with 1.0 M methanol at a feed rate of  $5 \text{ ml min}^{-1}$ . The shallowest channel (0.3 mm) exhibits a more or less similar performance to that of the deepest channel (1.0 mm) that has the same linear velocity, despite the fact that the volumetric flow rate of the 0.3 mm channel is only three-tenths of that of the 1.0 mm channel. The impedance spectra shown in Fig. 6(b) also do not show any appreciable differences to that in Fig. 5(b).



**Fig. 6.** (a) Effect of cathode channel depth and linear velocity on performance of single cell at  $80^\circ\text{C}$  and (b) electrochemical impedance analysis for single cell at  $80^\circ\text{C}$ . Linear velocity is maintained at constant value of  $20.8 \text{ m s}^{-1}$  for all channel depths by controlling flow rates. One molar of methanol fed at rate of  $5 \text{ ml min}^{-1}$ .

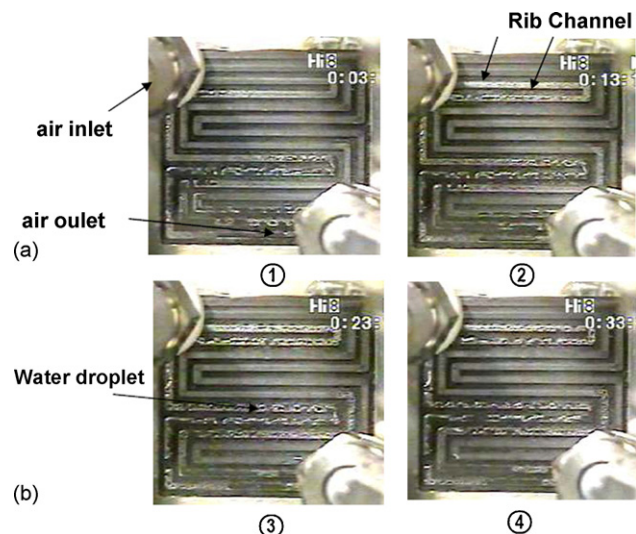


**Fig. 7.** Images of product water at cathodes and water removal behaviour with different channel depth of (a) 1.0 mm and (b) 0.5 mm. Operation current density is  $50 \text{ mA cm}^{-2}$  and 1.0 M methanol and dry air fed at rate of  $5 \text{ ml min}^{-1}$  and 100 sccm to anode and cathode, respectively. Pictures from left to right correspond to images at 0, 10, 20 and 30 min after start-up of cell.

This implies that the linear velocity can highly influence the performance of a cell; and the enhanced performance with the shallower channels can be attributed to the increased linear velocity.

The linear velocity may also affect the removal of the liquid water being produced at the cathode. The transport behaviour of water with respect to channel depth was monitored by using the transparent plates. A photograph of the test cell is presented in Fig. 2. Two different channel depths of 1.0 and 0.5 mm were used. The operating current density of the cell was fixed at  $50 \text{ mA cm}^{-2}$  and 1.0 M methanol and dry air were fed at a rate of  $5 \text{ ml min}^{-1}$  and 100 sccm to the anode and cathode, respectively. The behaviour of the product water in the channel was monitored with a video camera through the transparent plates. Photographs taken at every 10 min in sequence are presented in Fig. 7. The images from left to right were taken at the time interval of 0, 10, 20 and 30 min after start-up of the cell. Although the still photographs do not display water droplets as clearly as they appear in the movies, the continuous generation and movement of the water droplet in the channels can be seen to some extent (not shown here). Apparently, the removal of water in the 1.0 mm channel is not as efficient as that in the 0.5 mm channel, where fast removal can be observed (see Fig. 7). The efficient removal of water in the shallowest channel possibly minimizes the resistance of air flow in the channel as well as clearing water droplets from the electrode surfaces [16], and there by enhancing the performance of the cell.

As seen in Figs. 3 and 4, a pressure drop ( $\Delta P$ ) exists inside the channels and is directly affected by the channel depth. In order to understand the effect of  $\Delta P$  on the performance of a cell in a more precise manner, the cell was artificially pressurized to have the same internal pressure as those of the cells with different channel depths. The performance of a cell with a 1.0 mm channel depth was measured, while the internal pressure was raised to 2.6, 4, 10 and 29 kPa (gauge pressure) by controlling a needle valve at the cathode outlet. These pressures correspond to an internal pressure of 2.6, 3.9, 10.2 and 29.0 kPa for cells with a channel depth of 1.0, 0.8, 0.5 and 0.3 mm, respectively. The performance of a cell with respect to the internal pressures is shown in Fig. 8. It is clear that the peak powers linearly increase with internal pressure. This

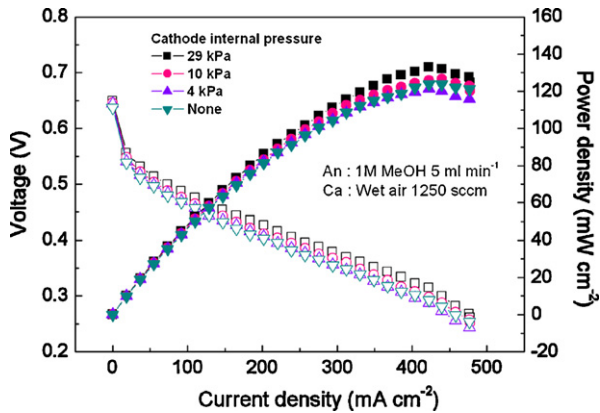


Fig. 8. Effect of cathode backpressure on performance of single cell at 80 °C at fixed cathode channel depth of 1.0 mm. One molar of methanol and 65 °C wet air were at rate of 5 ml min<sup>-1</sup> and 1250 sccm to anode and cathode, respectively.

shows that increased internal pressure has a positive impact on cell performance, which may be due to an increase in the partial pressure of oxygen. According to the Hagen–Poiseuille equation [23],  $\Delta P$  is inversely proportional to the square of the channel depth, and therefore a slight decrease in channel depth can lead to a huge increase in the pressure drop, i.e., 2.5 kPa at 1.0 mm vs. 28.5 kPa at 0.3 mm, which was measured with an electric manometer (477-3-FM, Dwyer) directly connected to the inlet and outlet of the cell. The increase in  $\Delta P$  is probably one of the reasons for the improvement in the performance of the cell with shallower channels:

$$E - E^0 = -\frac{RT}{6F} \ln \left( \frac{P_{\text{H}_2\text{O}}^2 P_{\text{CO}_2}}{P_{\text{CH}_3\text{OH}} P_{\text{O}_2}^{3/2}} \right) \quad (3)$$

$$E - E^0 = -\frac{RT}{6F} \ln \left( \frac{P_{\text{H}_2\text{O}}^2 P_{\text{CO}_2}}{P_{\text{CH}_3\text{OH}}} \right) - \frac{RT}{6F} \ln \left( \frac{1}{P_{\text{O}_2}^{3/2}} \right) \quad (4)$$

$$V_2 - V_1 = \frac{RT}{6F} \ln \left( \frac{P_2}{P_1} \right) \quad (V = E - E^0) \quad (5)$$

For the overall DMFC reaction, as per the Nernst equation (Eqs. (3) and (4)), the increased  $\Delta P$  can lead to an increase in the partial pressure of oxygen [25,26], and thus the performance of a cell with a shallower channel (which has a higher  $\Delta P$ ) is found to be increased. According to Eq. (5), while the pressure drop in the cathode is over 10 times between 0.3 and 1.0 mm channels, the voltage of the cell is slightly increased by 0.012 V at a fixed current. Hence, it is inferred that the combined effects of the increased linear velocity and internal pressure are responsible for the enhancement in cell performance.

Water removal from the channels has a direct impact on the stability of the performance during the course of operation of a cell. Cell performance as a function of cathode channel depth with two different air stoichiometries ( $\lambda = 5$  and 3) is presented in Fig. 9. The stoichiometry is fixed at a given value for each current density by controlling the flow rate. For  $\lambda = 5$  (as the current is changed, the flow rate will also change), the performance of a cell is found to be the highest with a 0.3 mm depth, and it gradually decreases with increasing depth of the channel. For all channel depths, the cells exhibit stable current–voltage ( $I$ – $V$ ) behaviour without being subjected to any fluctuations. At a relatively low flow rate (in case of  $\lambda = 3$ ), however, the  $I$ – $V$  curve has scattered data points for 1.0 mm depth that implies the fact that the unstable  $I$ – $V$  behaviour occurred during operation of a cell. This could be due to the uneven distribution of the reactants and the inadequate momentum needed to

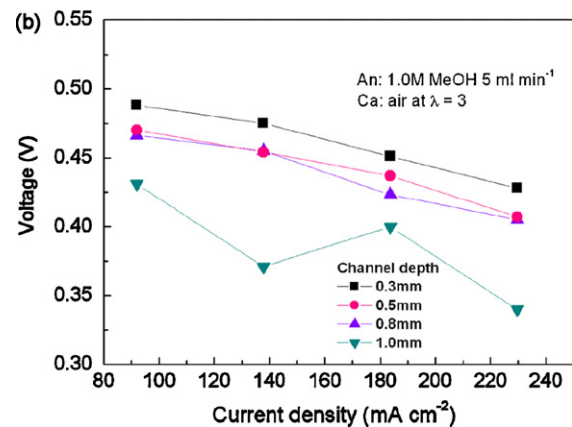
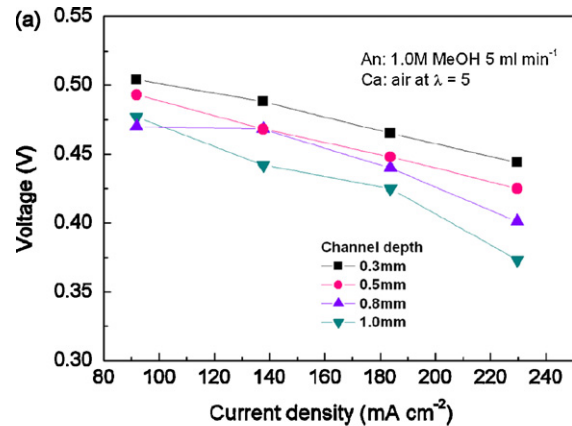


Fig. 9. Performance of single cell at 80 °C with cathode channel depth varying from 0.3 to 1.0 mm at two different stoichiometries: (a)  $\lambda = 5$  and (b)  $\lambda = 3$ . In both cases, 1.0M methanol fed at rate of 5 ml min<sup>-1</sup>.

push away the product water under the situation of low flow rate in the case of deeper channels, where the linear velocity of air is lower.

The effect of channel depth towards the stability of the cell performance is shown by continuous experiments conducted at a constant current. Fig. 10 shows the voltage–time curves of the cells with different channel depths obtained at a constant electric load of 100 mA cm<sup>-2</sup> with a fixed  $\lambda$  of 2 for both the anode and the cathode.

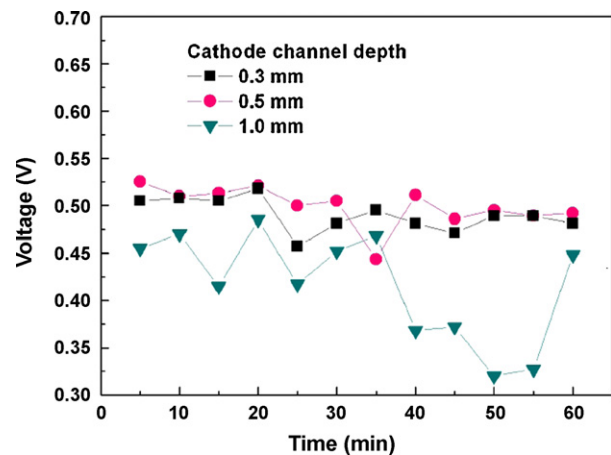


Fig. 10. Chronopotentiometric responses of single cells (operated at 80 °C) as function of cathode channel depth under constant current of 100 mA cm<sup>-2</sup>. One molar of methanol and dry air fed at rate of 0.2 ml min<sup>-1</sup> and 33 sccm to anode and cathode, respectively.

Cells with shallower channel depths, i.e., 0.3 and 0.5 mm exhibit a stable performance even at this low flow rate. On the other hand, the cell with a 1.0 mm channel experiences a severe voltage fluctuation as time passes. Obviously, factors such as inefficient mass transport and water removal are responsible for the unstable performance during the operation of cells with deeper channels.

#### 4. Conclusions

In the present investigation, the impact of the cathode channel depth on the performance of a DMFC has been investigated in a detailed manner. By using a single cell, a brief simulation has been conducted to identify the changes that take place in the linear velocity and pressure drop in the cathode channels. When the channel depth is decreased from 1.0 to 0.3 mm, the cell performance increases in a linear manner. From the experimental findings, it has been ascertained that two factors, namely, linear velocity and internal pressure, for shallower channels are responsible for enhancement of the mass transport of air/water and an increase in oxygen partial pressure inside the channel that, in turn, can contribute to the improvement in the performance as well as the stable operating condition of a cell. The reduction in the channel depth can render a better performance and also helps to reduce the total volume of the fuel cell stack, both of which are highly beneficial in raising the volumetric power density of the stack.

#### Acknowledgements

This study was supported by the Korea National RD&D Organization For Hydrogen & Fuel Cell and the Ministry of Commerce, Industry and Energy under contract number 2006-N-FC12-P-03-3-020-2007.

#### References

- [1] R. Dillon, S. Srinivasan, A.S. Aricò, V. Antonucci, J. Power Sources 127 (2004) 112–126.
- [2] J.C. Amphlett, B.A. Peppley, H. Ela, S. Aamir, J. Power Sources 96 (2001) 204–213.
- [3] M.A.J. Cropper, S. Geiger, D.M. Jollie, J. Power Sources 131 (2004) 57–61.
- [4] G.Q. Lu, C.Y. Wang, J. Power Sources 134 (2004) 33–40.
- [5] K. Scott, P. Argyropoulos, P. Yiannopoulos, W.M. Taama, J. Appl. Electrochem. 31 (2001) 823–832.
- [6] A.S. Aricò, P.L. Antonucci, E. Modica, V. Baglio, H. Kim, V. Antonucci, Electrochim. Acta 47 (2002) 3723–3732.
- [7] V. Neburchilov, J. Martin, H. Wang, J. Zhang, J. Power Sources 169 (2007) 221–238.
- [8] B. Bae, D. Kim, H.-J. Kim, T.-H. Lim, I.-H. Oh, H.Y. Ha, J. Phys. Chem. B 110 (2006) 4240–4246.
- [9] C. Xu, T.S. Zhao, Y.L. He, J. Power Sources 171 (2007) 268–274.
- [10] S.Q. Song, Z.X. Liang, W.J. Zhou, G.Q. Sun, Q. Xin, V. Stegiopoulos, P. Tsiakaras, J. Power Sources 145 (2005) 495–501.
- [11] H. Dohle, R. Jung, N. Kimiaie, J. Mergel, M. Muller, J. Power Sources 124 (2003) 371–384.
- [12] A.S. Aricò, P. Creti, V. Baglio, E. Modica, V. Antonucci, J. Power Sources 91 (2000) 202–209.
- [13] C. Xu, T.S. Zhao, Electrochem. Commun. 9 (2007) 497–503.
- [14] H. Yang, T.S. Zhao, Electrochim. Acta 50 (2005) 3243–3252.
- [15] C.W. Wong, T.S. Zhao, Q. Ye, J.G. Liu, J. Power Sources 155 (2006) 291–296.
- [16] C.W. Wong, T.S. Zhao, Q. Ye, J.G. Liu, J. Electrochem. Soc. 152 (2005) A1600.
- [17] H. Yang, T.S. Zhao, Q. Ye, Electrochem. Commun. 6 (2004) 1098–1103.
- [18] Y.G. Yoon, W.Y. Lee, G.G. Park, T.H. Yang, C.S. Kim, Int. J. Hydrogen Energy 30 (2005) 1363–1366.
- [19] D. Kim, M.A. Scibioh, S. Kwak, I.-H. Oh, H.Y. Ha, Electrochem. Commun. 6 (2004) 1069–1074.
- [20] D. Kim, J. Lee, T.-H. Lim, I.-H. Oh, H.Y. Ha, J. Power Sources 155 (2006) 203–212.
- [21] P. Argyropoulos, K. Scott, W.M. Taama, J. Appl. Electrochem. 29 (1999) 663–671.
- [22] C.Y. Chen, J.Y. Shiu, Y.S. Lee, J. Power Sources 159 (2006) 1042–1047.
- [23] W.L. McCabe, J.C. Smith, P. Harriott, Unit Operations of Chemical Engineering, sixth ed., McGraw-Hill, New York, 2001, pp. 99–100.
- [24] E. Arato, M. Pinna, P. Costa, J. Power Sources 158 (2006) 206–212.
- [25] S.-S. Hsieh, S.-H. Yang, J.-K. Kuo, C.-F. Huang, H.-H. Tsai, Energy Convers. Manage. 47 (2006) 1868–1878.
- [26] J. Larminie, A. Dicks, Fuel Cell Systems Explained, second ed., Wiley, Chichester, 2003, pp. 35–42.